# A characterization of quantum chaos by two-point correlation functions

Hrant Gharibyan, Masanori Hanada, Rian Swingle, and Masaki Tezuka<sup>5</sup>

<sup>1</sup>Stanford Institute for Theoretical Physics, Stanford University, Stanford, CA 94305, USA

<sup>2</sup>School of Physics and Astronomy, and STAG Research Centre,

University of Southampton, Southampton, SO17 1BJ, UK

<sup>3</sup>Department of Physics, Brown University, 182 Hope Street, Providence, RI 02912, USA

<sup>4</sup>Condensed Matter Theory Center, Maryland Center for Fundamental Physics,

Joint Center for Quantum Information and Computer Science,
and Department of Physics, University of Maryland, College Park MD 20742, USA

<sup>5</sup>Department of Physics, Kyoto University, Kyoto 606-8502, Japan

We propose a characterization of quantum many-body chaos: given a collection of simple operators, the set of all possible pair-correlations between these operators can be organized into a matrix with random-matrix-like spectrum. This approach is particularly useful for locally interacting systems, which do not generically show exponential Lyapunov growth of out-of-time-ordered correlators. We demonstrate the validity of this characterization by numerically studying the Sachdev-Ye-Kitaev model and a one-dimensional spin chain with random magnetic field (XXZ model).

### INTRODUCTION

How do we characterize quantum chaos? Among a wide variety of different approaches (see [1] for a review), two rather different criteria are currently in wide use. The first one is random-matrix-like universality of the fine-grained energy spectrum [2, 3]: a given quantum system is chaotic in this sense if the fine-grained energy spectrum is described by Random Matrix Theory (RMT) [4–6]. The second one is sensitivity to initial conditions: a given quantum system is chaotic in this sense if it exhibits exponential Lyapunov growth of a small perturbation as probed by an out-of-time-order correlation function (OTOC) [7, 8]. OTOCs are closely related to Loschmidt echoes which also probe chaos [9].

There are several unsatisfactory features regarding these criteria. First, it is unclear how the two criteria are related. Second, the connection of the quantum criteria to the characterizations of classical chaos are unclear. One might expect that sensitivity to initial conditions can characterize both classical and quantum chaos, but there is a problem for local quantum systems. In the classical theory, the initial perturbation can be taken arbitrarily small in the mathematical sense, and the exponential growth can continue forever. On the other hand, in a quantum system the perturbation cannot be arbitrarily small due to the uncertainty principle, and local quantum systems do not generally show exponential growth except in special limits [10–14]. [15] Hence, the characterization based on the early growth of OTOCs does not work for generic local quantum systems.

In a previous paper [16], we generalized the above single chaos exponent to define a spectrum of quantum Lyapunov exponents. Based on calculations in the Sachdev-Ye-Kitaev (SYK) model and a spin chain (XXZ) model, we proposed that the Lyapunov exponents so defined exhibit a universal behavior: the fine-grained Lyapunov spectrum agrees with RMT when the system is chaotic. This characterization of quantum chaos circumvented the problem of lack of exponential growth in generic local systems, since one needs only the statistical property of the exponents instead of their detailed growth behavior. Because RMT behavior in the Lyapunov spectrum coincides with RMT behavior in the energy spectrum for the models we considered, the Lyapunov spectrum may be useful for connecting the different criteria for chaos. As a bouns, universality in the quantum Lyapunov spectrum has a classical counterpart [17], so it may also be useful to connect classical and quantum chaos.

We emphasize that these universalities are merely empirical. There may be other observables that provide a similar characterization of quantum chaos which are also more accessible to experiment. In this paper, we consider time-ordered two-point correlators that are easier to study, both theoretically and experimentally, than OTOCs. Specifically, given a set of simple operators  $\{O_j\}$ , we consider the matrix of all possible two-point functions  $\langle O_i(t)O_j(0)\rangle$  where  $O(t)=e^{iHt}Oe^{-iHt}$ , construct its time-dependent spectrum, and then study the statistical properties of the spectrum. Based on

this study, we propose that this two-point correlation spectrum, which is roughly a spectrum of decay rates, has universal statistical properties for all chaotic systems.

Below, we first define the two models, SYK and XXZ, that we will consider. Next, we define a spectrum of decay rates derived from two-point functions and propose a universal behavior for the spectrum in chaotic systems. Then we provide detailed numerical evidence for the conjecture using finite size exact diagonalization studies.

# **MODELS**

The first example is the SYK model [18–20] (see Ref. [21] for a recent review) consisting of N Majorana fermions with Hamiltonian

$$\hat{H} = \sqrt{\frac{6}{N^3}} \sum_{i < j < k < l} J_{ijkl} \hat{\psi}_i \hat{\psi}_j \hat{\psi}_k \hat{\psi}_l + \frac{\sqrt{-1}}{\sqrt{N}} \sum_{i < j} K_{ij} \hat{\psi}_i \hat{\psi}_j.$$

$$(1)$$

Majorana fermions satisfy the anti-commutation relations  $\{\hat{\psi}_i, \hat{\psi}_j\} = \delta_{ij}$  and  $J_{ijkl}$  is random Gaussian coupling with mean zero and standard deviation 1. The energy also includes a quadratic term, and  $K_{ij}$  is Gaussian random with mean zero and standard deviation K. The dimension of the Hilbert space is  $2^{N/2}$ . When K=0, this model is maximally chaotic at low temperatures, namely the MSS bound [18, 20] is asymptotically saturated. When K>0, low-energy modes become non-chaotic, while high-energy modes remain chaotic [22, 23].

The second example is the XXZ model, a onedimensional S=1/2 spin chain with random magnetic field along z-direction (see e.g. [24]),

$$\hat{H} = \sum_{i=1}^{N_{\text{site}}} \left( \frac{1}{4} \vec{\sigma}_i \vec{\sigma}_{i+1} + \frac{w_i}{2} \sigma_{z,i} \right). \tag{2}$$

Here  $\vec{\sigma} = (\sigma_x, \sigma_y, \sigma_z)$  are Pauli matrices with periodic boundary condition  $\vec{\sigma}_{N_{\rm site}+1} = \vec{\sigma}_1$ . The random magnetic fields  $w_i$  are independent and uniformly distributed in [-W, +W]. At  $W \gtrsim 3.5$ , most of the energy eigenstates are in the many-body localized (MBL) phase [24, 25]. (For the physics of the MBL phase, see e.g. [26–29].)

### **PROPOSAL**

The starting point is choosing a set of operators and organizing the set of two-point functions into a matrix. The matrix of two-point functions,  $G_{ij}^{(\phi)}(t)$ , is defined by

$$G_{ij}^{(\phi)}(t) = \langle \phi | \hat{\psi}_i(t) \hat{\psi}_j(0) | \phi \rangle \tag{3}$$

for SYK, and by

$$G_{ij}^{(\phi)}(t) = \langle \phi | \sigma_{+,i}(t) \sigma_{-,j}(0) | \phi \rangle \tag{4}$$

for XXZ, where  $\sigma_{\pm} = \frac{\sigma_x \pm i \sigma_y}{2}$ . Here, we will take the state  $|\phi\rangle$  to be an energy eigenstate, but this is not essential as explained in the discussion. Note also that we can consider other two-point functions, e.g.  $G_{ij}^{(\phi)}(t) = \langle \phi | \sigma_{z,i}(t) \sigma_{z,j}(0) | \phi \rangle$ ; the generalization to other systems is straightforward.

Let the singular values of  $G_{ij}^{(\phi)}(t)$  be  $e^{\lambda_i^{(\phi)}(t)}$ . We denote the  $\lambda_i^{(\phi)}(t)$  as 'exponents'. Our conjecture is two-fold:

- In quantum chaotic systems,  $G_{ij}^{(\phi)}$  becomes 'random' at sufficiently large t. Namely, in the chaotic theories the exponents are described by RMT.
- In non-ergodic theories (e.g. the MBL phase) the exponents are not described by RMT.

The idea behind this conjecture is simple. When the system is chaotic, the information about the local perturbation should be washed away. Hence it is natural to expect that  $G_{ij}^{(\phi)}(t)$  becomes a random matrix. On the other hand, if the system is not chaotic, some structure should survive and a deviation from RMT should be observable.

How this characterization is related to other characterizations, such as RMT universality in the energy spectrum or the exponential Lyapunov growth of OTOCs, is not clear at this moment. Below, we at least demonstrate that these characterizations are compatible in the SYK and XXZ models.

### NUMERICAL STUDY

In this section, we calculate the exponents  $\lambda_i^{(\phi)}(t)$  numerically and study their statistical features. The exponents are sorted such that  $\lambda_i^{(\phi)}(t) \geq$   $\lambda_2^{(\phi)}(t) \geq \cdots \geq \lambda_N^{(\phi)}(t)$ . The primary objects of study are the nearest-neighbor level separation  $s_i^{(\phi)}(t) \equiv \lambda_i^{(\phi)}(t) - \lambda_{i+1}^{(\phi)}(t)$  and the nearest-neighbor gap ratio  $r_i = \frac{\min(s_i, s_{i+1})}{\max(s_i, s_{i+1})}$ . Because the number of exponents we can obtain numerically is small, we need to use the fixed-i unfolding method [16] (see appendix for details).

Consider first the SYK model. When  $|\phi\rangle$  is energy eigenstate, then unless K=0 and N mod 8 is zero,  $G_{ij}^{(\phi)}(t)$  is a complex matrix without particular symmetry. Hence, when the system is chaotic, if RMT behavior emerges, the relevant ensemble would be the Gaussian unitary ensemble (GUE). When K=0 and N mod 8 is zero,  $G_{ij}^{(\phi)}(t)$  is complex and symmetric and in this case one expects Gaussian orthogonal ensemble (GOE) statistics. Hence we expect GOE when  $K\simeq 0$  and N mod 8 is zero.

At the values of N we study, the energy dependence of the spectrum is not large. (The energy dependence is similar to the case of the Lyapunov spectrum; see [16] for a detailed explanation.) Hence, it is simplest to average over all energy eigenstates. Numerically we find that the gap between  $\lambda_{N/2}$  and  $\lambda_{N/2+1}$  is bigger than the other gaps and appears to behave differently when K is large, as explained in more detail in the supplementary material. Hence, we use only the first half of the spectrum with N/2 exponents in the analysis. We checked that similar results are obtained using the other half of the spectrum.

Fig. 1 shows the nearest-neighbor level separation. Near K=0 (chaotic phase) the spectrum is GUE-like. [30] It is interesting that the GUE behavior can be seen at all time scales. We observed the same phenomenon for other  $N\not\equiv 0$  mod 8. For  $N\equiv 0$  mod 8, the spectrum is GOE-like at sufficiently late time, but at early time there are large deviations from GOE. In the opposite limit of large K, in which the system is not chaotic to leading order, the spectrum is Poisson-like. This claim is substantiated in Fig. 2 which shows the nearest-neighbor gap ratio. The GUE value is approximately obtained when  $K\simeq 0$ , while at large K the ratio is close to the Poisson value.

Now consider the XXZ model. This model conserves the z-component of the total spin, and we consider only the  $S^z = 0$  sector. We study two values of the W parameter, W = 0.5 (the ergodic phase) and W = 4 (the MBL phase). In this

model,  $G^{(\phi)}$  is complex and symmetric when  $|\phi\rangle$  is an energy eigenstate (see supplementary material). Hence, in the ergodic phase, we expect GOE statistics.

To orient the discussion, we first discuss the time-scale for the decay of the two-point functions. For W=4, we observe a clear split of the larger and smaller halves. Hence, the larger half of the exponents is used for the analysis, both for W=0.5 and for W=4. We checked that the result does not change much if the smaller half, or all the exponents, are used provided  $N_{\rm site}$  is large enough  $(N_{\rm site}=12,14)$ .

The energy dependence is rather large unlike the SYK model. (Again, see [16] for a detailed explanation.) Hence we need to restrict the energy to be in a small range in order to remove an uncontrolled energy variation from the analysis.

Fig. 3 shows the distribution of the nearest-neighbor level separation. The chaotic phase exhibits a GOE distribution, while the distribution is close to Poisson in the MBL phase. Note that, unlike the SYK model, the chaotic phase is not described by RMT at early time. Interestingly, the deviation from RMT becomes large at  $1 \lesssim t \lesssim 10$ , but it eventually vanishes. [31] There is a curious  $N_{\rm site}$ -dependence of this deviation at intermediate time which is discussed further in the supplementary material.

In Fig. 4 the averaged nearest-neighbor gap ratio is plotted. In the chaotic phase (W=0.5), the value of  $\langle r \rangle$  is not strongly dependent on t and approaches the GOE value [32]. The agreement with the GOE value even at intermediate time is likely a coincidence, because the nearest-neighbor level separation is not close to GOE. In the MBL phase (W=4),  $\langle r \rangle$  is smaller than the GOE value and decreases toward the Poisson value as N increases.

# SUMMARY AND DISCUSSION

Here we introduced a spectrum defined from a matrix of two-point functions ((3) for SYK and (4) for XXZ), and proposed that the statistical features of this spectrum exhibit random matrix universality when the underlying system is chaotic.

While we have used the energy eigenstates to define the spectrum, this particular choice is not crucial to observe universality. Spin eigenstates such as  $|\uparrow\uparrow\cdots\uparrow\uparrow\rangle$  and  $|\uparrow\downarrow\cdots\uparrow\downarrow\rangle$  also yield the same struc-

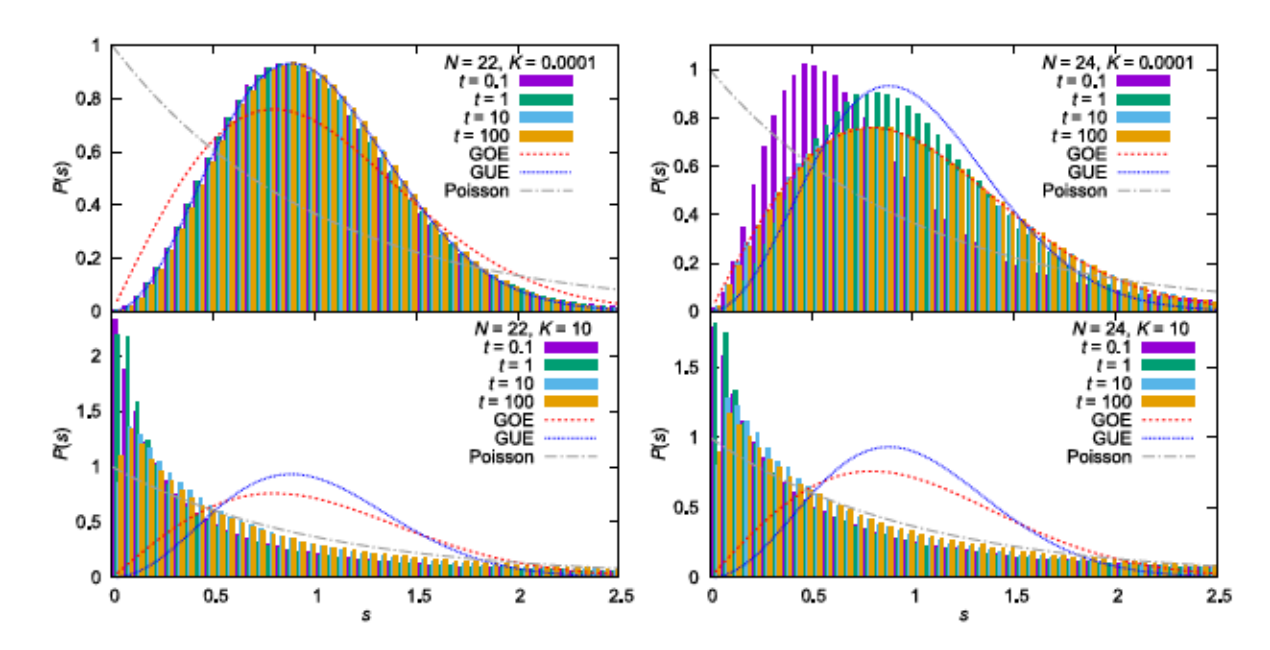


FIG. 1. SYK, the distribution of nearest neighbor level separation for various values of t, K = 0.0001 and K = 10. All eigenstates are used and the larger N/2 exponents are used. N = 22, 24.

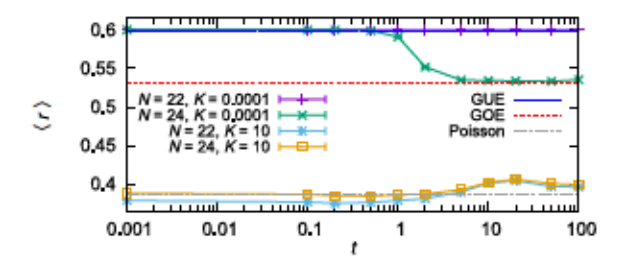


FIG. 2. SYK, the time dependence of nearest neighbor gap ratio  $\langle r \rangle$  for N=22 and 24, K=0.0001 and K=10.2000 (16) samples are used for N=22 (24).

ture [33] at long time, but the time-scale for the onset of RMT-behavior can depend on the choice of state.

In this paper, all the models considered have some degree of disorder in their definition. One could worry that this disorder is the source of the RMT behavior. The fact that we do not observe RMT signatures in the MBL phase shows that this is not so. However, given a theory without disorder and a highly symmetric state  $|\phi\rangle$ , the RMT behavior may not be visible. In the case of a chaotic system without disorder, we conjecture that, if randomness is introduced in the choice of  $|\phi\rangle$ , then RMT behavior

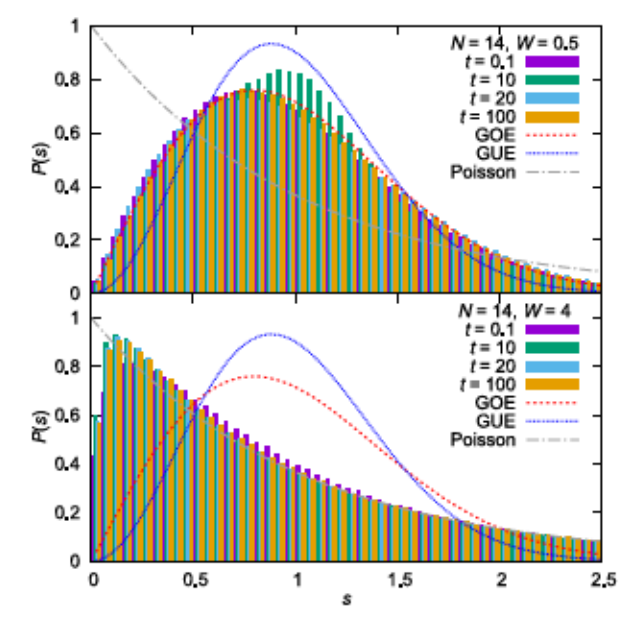


FIG. 3. The distribution of nearest-neighbor level separation s, XXZ, t=0.1,10,20,100 for W=0.5 and W=4, with  $N_{\rm site}=14$  for central 10 % of the energy eigenstates. The largest  $N_{\rm site}/2$  exponents are used. The technical details of the fixed-i unfolding and the  $N_{\rm site}$ -dependence are discussed in the supplementary material.

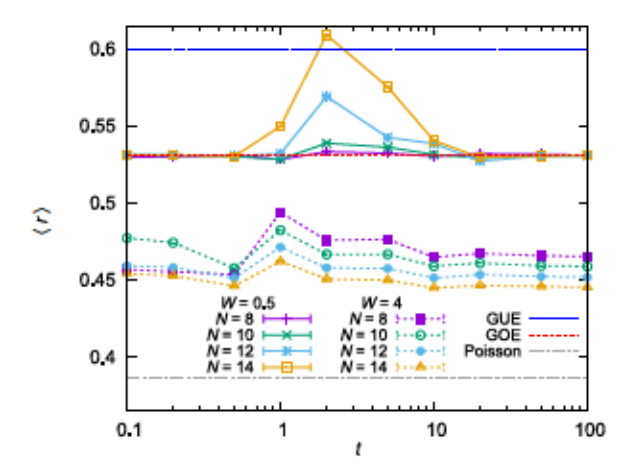


FIG. 4. The averaged nearest-neighbor gap ratio for the central 10 % of the energy eigenstates. At least 22000 (1200) samples are used for  $N_{\rm site} = 12, 10, 8$ ( $N_{\rm site} = 14$ ). The largest  $N_{\rm site}/2$  exponents are used.

### will be observed.

There are various generalizations and extensions of this work. One clear task is to see if the same signatures are observed in other chaotic models. Another goal is an analytic argument for the observed behavior. One can also consider Euclidean two-point functions, which are more accessible in a variety of systems thanks to Monte Carlo methods. If RMT universality can be observed there, it would provide a powerful tool to study the chaotic nature of large systems where real-time dynamics is hard to access numerically. The matrix of two-point functions considered here can be defined in classical systems as well. Whether the same universality can be found in that context is another interesting question.

# ACKNOWLEDGMENTS

We thank S. Hikami, S. Matsuura and H. Shimada for stimulating discussions. This work was partially supported by JSPS KAKENHI Grants 17K14285 (M. H.) and 17K17822 (M. T.), the Simons Foundation via the It From Qubit Collaboration (B. S.), and the Department of Energy award number de-sc0017905 (B. S). H. G. was supported in part by NSF grant PHY-1720397. M. H. thanks Brown University for the hospitality during his stay while completing the paper, and acknowledges the STFC Ernest Rutherford Grant ST/R003599/1.

- L. D'Alessio, Y. Kafri, A. Polkovnikov, and M. Rigol, "From quantum chaos and eigenstate thermalization to statistical mechanics and thermodynamics," Advances in Physics 65 (May, 2016) 239-362, arXiv:1509.06411 [cond-mat.stat-mech].
- [2] O. Bohigas, M. J. Giannoni, and C. Schmit, "Characterization of chaotic quantum spectra and universality of level fluctuation laws," *Phys. Rev.* Lett. 52 (Jan, 1984) 1-4. https://link.aps.org/ doi/10.1103/PhysRevLett.52.1.
- [3] F. Haake, Quantum signatures of chaos, vol. 54. Springer Science & Business Media, 2013.
- [4] E. P. Wigner, "Characteristic vectors of bordered matrices with infinite dimensions i," in *The* Collected Works of Eugene Paul Wigner, pp. 524-540. Springer, 1993.
- [5] F. J. Dyson, "Statistical theory of the energy levels of complex systems. i," *Journal of Mathematical Physics* 3 no. 1, (1962) 140–156.
- [6] M. L. Mehta, Random matrices, vol. 142. Elsevier, 2004
- [7] A. Larkin and Y. N. Ovchinnikov, "Quasiclassical method in the theory of superconductivity," Sov Phys JETP 28 no. 6, (1969) 1200-1205.
- [8] A. Almheiri, D. Marolf, J. Polchinski, D. Stanford, and J. Sully, "An Apologia for Firewalls," *JHEP* 09 (2013) 018, arXiv:1304.6483 [hep-th].
- [9] A. Goussev, R. A. Jalabert, H. M. Pastawski, and D. Wisniacki, "Loschmidt Echo," arXiv e-prints (Jun, 2012) arXiv:1206.6348, arXiv:1206.6348 [nlin.CD].
- [10] A. Nahum, S. Vijay, and J. Haah, "Operator Spreading in Random Unitary Circuits," *Physical Review X* 8 (Apr. 2018) 021014, arXiv:1705.08975 [cond-mat.str-el].
- [11] C. W. von Keyserlingk, T. Rakovszky, F. Pollmann, and S. L. Sondhi, "Operator Hydrodynamics, OTOCs, and Entanglement Growth in Systems without Conservation Laws," Physical Review X 8 (Apr, 2018) 021013, arXiv:1705.08910 [cond-mat.str-el].
- [12] S. Xu and B. Swingle, "Accessing scrambling using matrix product operators," arXiv e-prints (Feb, 2018) arXiv:1802.00801, arXiv:1802.00801 [quant-ph].
- [13] S. Xu and B. Swingle, "Locality, Quantum Fluctuations, and Scrambling," arXiv e-prints (May, 2018) arXiv:1805.05376, arXiv:1805.05376 [cond-mat.str-el].
- [14] V. Khemani, D. A. Huse, and A. Nahum, "Velocity-dependent Lyapunov exponents in

- many-body quantum, semiclassical, and classical chaos," *Physical Review B* **98** (Oct, 2018) 144304, arXiv:1803.05902 [cond-mat.stat-mech].
- [15] In the context of holography, the large-N limit of a gauge theory, a vector model, or the SYK model are often considered. In these examples, N corresponds to the number of the internal degrees of freedom. These internal interactions can be regarded as highly non-local in the sense that all of them interact directly with each other. Large N also plays the role of small  $\hbar$ , giving a kind of semi-classical limit. In these cases, the exponential growth of OTOC is a good indicator of chaos.
- [16] H. Gharibyan, M. Hanada, B. Swingle, and M. Tezuka, "Quantum Lyapunov Spectrum," arXiv:1809.01671 [quant-ph].
- [17] M. Hanada, H. Shimada, and M. Tezuka, "Universality in Chaos: Lyapunov Spectrum and Random Matrix Theory," *Phys. Rev.* E97 no. 2, (2018) 022224, arXiv:1702.06935 [hep-th].
- [18] J. Maldacena and D. Stanford, "Remarks on the Sachdev-Ye-Kitaev model," Phys. Rev. D94 no. 10, (2016) 106002, arXiv:1604.07818 [hep-th].
- [19] S. Sachdev, "Bekenstein-Hawking Entropy and Strange Metals," Phys. Rev. X5 no. 4, (2015) 041025, arXiv:1506.05111 [hep-th].
- [20] A. Kitaev, "A simple model of quantum holography, Part 1 and Part 2 (talks at KITP, Santa Barbara),".
- [21] V. Rosenhaus, "An introduction to the SYK model," arXiv:1807.03334 [hep-th].
- [22] A. M. Garcia-Garcia, B. Loureiro, A. Romero-Bermudez, and M. Tezuka, "Chaotic-Integrable transition in the Sachdev-Ye-Kitaev model," *Phys. Rev. Lett.* 120 (2018) 241603, arXiv:1707.02197 [hep-th].
- [23] T. Nosaka, D. Rosa, and J. Yoon, "Thouless time for mass-deformed SYK," JHEP 09 (2018), arXiv:1804.09934 [hep-th].
- [24] D. J. Luitz, N. Laflorencie, and F. Alet, "Many-body localization edge in the random-field heisenberg chain," *Phys. Rev. B* **91** (Feb, 2015) 081103. https://link.aps.org/doi/10.1103/ PhysRevB.91.081103.
- [25] M. Serbyn, Z. Papic, and D. Abanin, "A criterion for many-body localization-delocalization phase transition, arxiv e-prints (2015)," arXiv preprint arXiv:1507.01635.
- [26] P. W. Anderson, "Absence of diffusion in certain random lattices," Phys. Rev. 109 (Mar, 1958) 1492-1505. https://link.aps.org/doi/10.1103/ PhysRev.109.1492.
- [27] I. V. Gornyi, A. D. Mirlin, and D. G. Polyakov, "Interacting electrons in disordered wires: Anderson localization and low-t transport," Phys. Rev. Lett. 95 (Nov, 2005) 206603. https://link.

- aps.org/doi/10.1103/PhysRevLett.95.206603.
- [28] D. Basko, I. Aleiner, and B. Altshuler, "Metalinsulator transition in a weakly interacting many-electron system with localized single-particle states," *Annals of Physics* **321** no. 5, (2006) 1126 – 1205. http://www.sciencedirect.com/science/article/pii/S0003491605002630.
- [29] I. L. Aleiner, B. L. Altshuler, and G. V. Shlyapnikov, "Finite temperature phase transition for disordered weakly interacting bosons in one dimension," *Nature Physics* 6 (2010) 900–904. https:
  - //hal.archives-ouvertes.fr/hal-00543657. 8 pages, 5 figures.
- [30] A small nonzero value K = 0.0001 is used to avoid a degeneracy in the energy spectrum when K is exactly zero.
- [31] The agreement is improved to some extent by removing the largest exponent, which decays much slower than others. Still, the deviation at short time remains.
- [32] Y. Y. Atas, E. Bogomolny, O. Giraud, and G. Roux, "Distribution of the ratio of consecutive level spacings in random matrix ensembles," *Phys. Rev. Lett.* **110** (Feb, 2013) 084101. https://link.aps.org/doi/10.1103/PhysRevLett.110.084101.
- [33] H. Gharibyan, M. Hanada, B. Swingle, and M. Tezuka, "In preparation,".
- [34] W. Fu and S. Sachdev, "Numerical study of fermion and boson models with infinite-range random interactions," *Phys. Rev.* **B94** no. 3, (2016) 035135, arXiv:1603.05246 [cond-mat.str-el].
- [35] Y.-Z. You, A. W. W. Ludwig, and C. Xu, "Sachdev-Ye-Kitaev Model and Thermalization on the Boundary of Many-Body Localized Fermionic Symmetry Protected Topological States," *Phys. Rev.* **B95** no. 11, (2017) 115150, arXiv:1602.06964 [cond-mat.str-el].
- [36] H. Gharibyan, M. Hanada, S. H. Shenker, and M. Tezuka, "Onset of Random Matrix Behavior in Scrambling Systems," *JHEP* 07 (2018) 124, arXiv:1803.08050 [hep-th].

### SUPPLEMENTARY MATERIAL

# Symmetry of $G_{ij}^{(\phi)}$

The matrix of two-point functions  $G_{ij}^{(\phi)}$  is usually a complex matrix without particular symmetry.

For the XXZ model,  $G_{ij}^{(\phi)}$  is complex and symmetric when the reference state is an energy eigenstate,  $|\phi\rangle = |E\rangle$ . To see this, first observe that the Hamiltonian is real and symmetric. Hence  $(e^{-iHt})^T = e^{-iHt}$ . Also, the energy eigenstates can be chosen to be real unit vectors (unless there is an accidental degeneracy in the energy spectrum, which does not happen for generic values of  $w_i$ 's), and hence,  $\langle E|\sigma_{+,i}(0) = (\sigma_{-,i}(0)|E\rangle)^T$ . Therefore,

$$\begin{split} G_{ij}^{(\phi)} &= \langle E|\sigma_{+,i}(t)\sigma_{-,j}(0)|E\rangle \\ &= e^{iEt}\langle E|\sigma_{+,i}(0)e^{-iHt}\sigma_{-,j}(0)|E\rangle \end{split}$$

is complex and symmetric.

Next let us consider the SYK model. The original Hamiltonian with K=0 exhibits different symmetry depending the value of  $N \mod 8$  — GOE for  $N\equiv 0$ , GUE for  $N\equiv 2,6$  and GSE for  $N\equiv 4$  [34, 35]. For  $N\equiv 0$  and  $N\equiv 4$  mod 8, the Hamiltonian can be taken to be real and symmetric. It can be seen by using the following representation:

$$\hat{\psi}_{1} = \sigma_{z} \otimes \mathbf{1} \otimes \mathbf{1} \otimes \mathbf{1} \otimes \cdots \otimes \mathbf{1} \otimes \mathbf{1}, 
\hat{\psi}_{2} = \sigma_{y} \otimes \sigma_{y} \otimes \sigma_{y} \otimes \sigma_{y} \otimes \cdots \otimes \sigma_{y} \otimes \sigma_{y}, 
\hat{\psi}_{3} = \sigma_{y} \otimes \sigma_{x} \otimes \mathbf{1} \otimes \sigma_{y} \otimes \cdots \otimes \sigma_{y} \otimes \sigma_{y}, 
\hat{\psi}_{4} = \sigma_{y} \otimes \sigma_{z} \otimes \mathbf{1} \otimes \sigma_{y} \otimes \cdots \otimes \sigma_{y} \otimes \sigma_{y}, 
\hat{\psi}_{5} = \sigma_{y} \otimes \sigma_{y} \otimes \sigma_{x} \otimes \mathbf{1} \otimes \cdots \otimes \sigma_{y} \otimes \sigma_{y}, 
\hat{\psi}_{6} = \sigma_{y} \otimes \sigma_{y} \otimes \sigma_{z} \otimes \mathbf{1} \otimes \cdots \otimes \sigma_{y} \otimes \sigma_{y}, 
\dots$$

$$\hat{\psi}_{N-3} = \sigma_{y} \otimes \sigma_{y} \otimes \sigma_{y} \otimes \sigma_{y} \otimes \cdots \otimes \sigma_{x} \otimes \mathbf{1}, 
\hat{\psi}_{N-2} = \sigma_{y} \otimes \sigma_{y} \otimes \sigma_{y} \otimes \sigma_{y} \otimes \cdots \otimes \sigma_{z} \otimes \mathbf{1}, 
\hat{\psi}_{N-1} = \sigma_{y} \otimes \mathbf{1} \otimes \sigma_{y} \otimes \sigma_{y} \otimes \cdots \otimes \sigma_{y} \otimes \sigma_{x}, 
\hat{\psi}_{N} = \sigma_{y} \otimes \mathbf{1} \otimes \sigma_{y} \otimes \sigma_{y} \otimes \cdots \otimes \sigma_{y} \otimes \sigma_{z}.$$
(5)

When  $N \equiv 0$  or 4 mod 8, they are all real and symmetric. (Note that  $\sigma_x$  and  $\sigma_z$  are real symmetric, while  $\sigma_y$  is pure imaginary and anti-symmetric.) Hence  $\hat{H} = \sqrt{\frac{6}{N^3}} \sum_{i < j < k < l} J_{ijkl} \hat{\psi}_i \hat{\psi}_j \hat{\psi}_k \hat{\psi}_l$  is real, and of course it is hermitian, and therefore, real and symmetric. Note that  $\hat{H}$  is not real when K is not zero.

When  $N \equiv 0$  and K = 0, the energy spectrum is not degenerate and the energy eigenstates are represented by real vectors. Therefore, just as in the case of the XXZ model, the matrix of two-point functions (3) is complex and symmetric for the energy eigenstates. Hence we expect the GOE statistics.

The situation is a little bit complicated when  $N\equiv 4$ , because the energy spectrum is two-fold degenerate. In general, an energy eigenstate is not a real vector, but rather, just a linear combination of two real vectors with complex coefficients. When we take K to be small but nonzero, the degeneracy is split, and the energy eigenstates are generically far from real vectors. Therefore, we expect the GUE statistics.

We can also see that  $G_{ij}^{(\phi)}(t=0)$  is real and symmetric when  $N\equiv 0$  and K=0. From this it follows that  $G_{ij}^{(\phi)}(0)=\frac{G_{ij}^{(\phi)}(0)+G_{ji}^{(\phi)}(0)}{2}=\frac{1}{2}\langle E|\{\hat{\psi}_i,\hat{\psi}_j\}|E\rangle=\frac{\delta_{ij}}{2}$ . Namely all exponents are  $-\log 2$  at t=0.

### Time dependence of the exponents $\lambda_i$

For the SYK model, in Fig. 5, the exponents  $\lambda_i(t)$  are plotted as functions of time t for K=0.0001,10 and various N. (When  $N\equiv 2$  or 6, it is possible to uniquely specify the energy eigenstates by taking into account parity as well [34, 35].) Note that, when  $N\equiv 0$  and  $K\simeq 0$ , all exponents are close to  $-\log 2$  at early time, as we have already explained. Presumably, this is the reason for the different early-time behaviors in the level statistics of  $N\equiv 0$  and  $N\equiv 2,4,6$ .

Next let us consider the XXZ model. In Fig. 6, the exponents  $\lambda_i(t)$  are plotted as functions of time t, for W = 0.5, 4 and  $N_{\text{site}} = 14$ . In the top panels, we have plotted all the exponents, by using 10% of the energy eigenstates in the middle of the spectrum. For W = 0.5, the largest exponent decays more slowly (decay time scale  $\sim 20$ ) than the other exponents (decay time scale  $\sim 10$ ). Due to this, a better agreement with RMT can be seen when we remove the largest exponent from the analysis of the statistical property. (Even with the largest exponent, the agreement with RMT is still good.) For W = 4, we can see a clear split of the larger and smaller halves. Hence we use the larger half for the analysis of the statistical property. (The result does not change much when we use the smaller half, or all exponents, at sufficiently large  $N_{\rm site}$ 

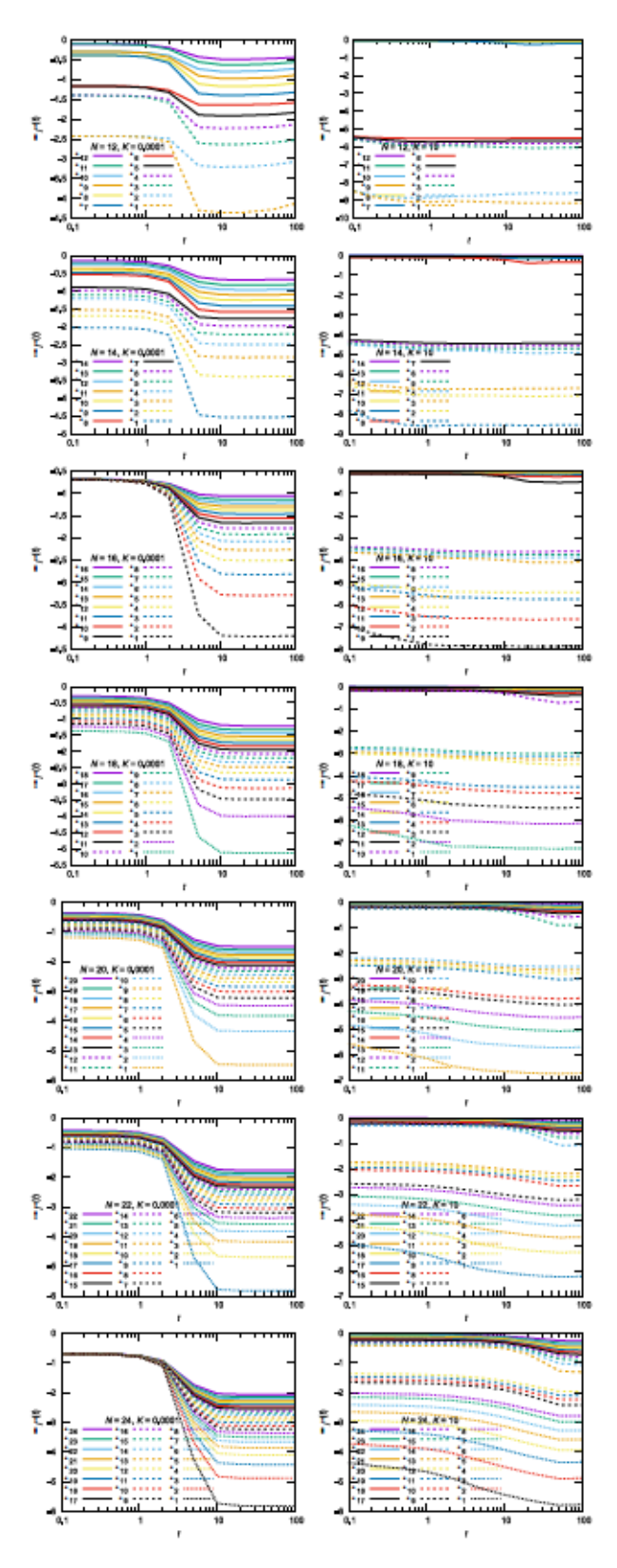


FIG. 5. SYK model, energy eigenstates, averaged exponents for K=0.0001 (left), K=10 for N=12,14,16,18,20,22,24 from top to bottom as functions of time t.

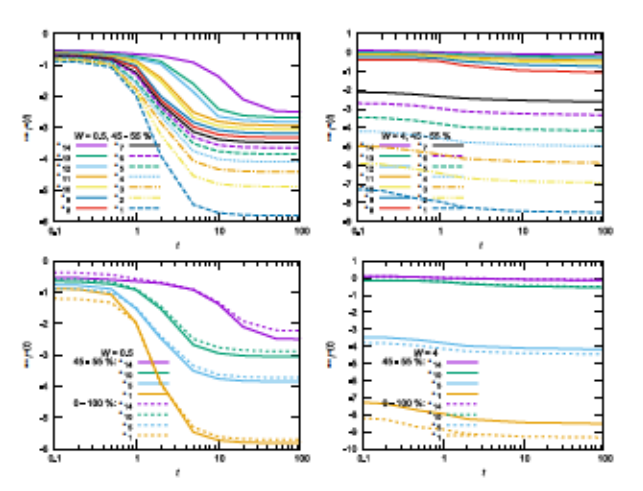


FIG. 6. XXZ model, energy eigenstates, averaged exponents for  $N_{\rm site} = 14$  and W = 0.5 (left), 4 (right) as functions of time t. Averages for the central 10% of the eigenstates (45 - 55%), shown in the upper row, and all the eigenstates (0 - 100%) are compared in the plots in the lower row for  $\lambda_1, \lambda_5, \lambda_{10}, \lambda_{14}$ .

 $(N_{\rm site}=12,14)$ .) In the bottom panels, we have compared the exponents calculated by using 10% of the energy eigenstates in the middle of the spectrum, and all the energy eigenstates. There are visible differences, and due to them, better agreement with RMT can be seen when the energy range is restricted.

### Details of unfolding

Because the number of exponents we can obtain numerically from each matrix of two-point functions is small, we need to use the fixed-i unfolding method [16]: for each i, we rescale  $s_i$  so that the average over many samples becomes 1. Namely, we take  $\tilde{s}_i = \frac{s_i}{\langle s_i \rangle}$ , where  $\langle \cdot \rangle$  stands for the average. We will call this  $\tilde{s}_i$  simply as  $s_i$  when there is no risk of confusion. The values of  $r_i$ 's shown below are calculated from these rescaled  $s_i$ 's.

In order to reduce finite-N effects further, we can use the sample-by-sample rescaling method as well. We shift the exponents so that the average becomes zero, and then rescale them so that the standard deviation becomes 1. Namely,  $\lambda_i^{(\phi)}(t) \mapsto \tilde{\lambda}_i^{(\phi)}(t) = \alpha \lambda_i^{(\phi)}(t) + \beta$  so that  $\sum_i \tilde{\lambda}_i^{(\phi)}(t) = 0$  and  $\sum_{i=1}^N \tilde{\lambda}_i^{(\phi)}(t)^2 = N$ . This can remove the N-dependent fluctuation of the entire width. When

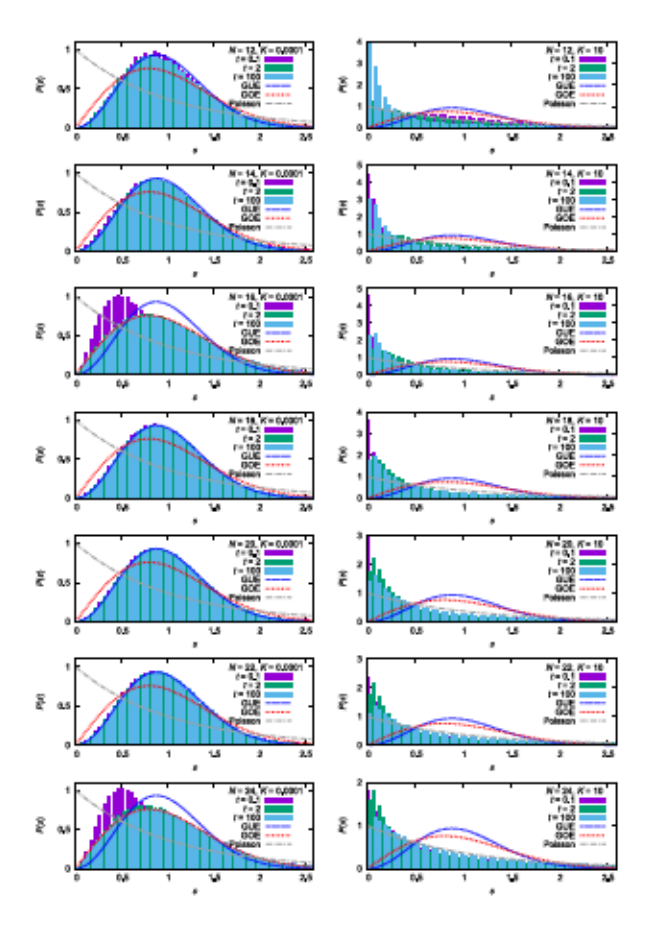


FIG. 7. The distribution of nearest-neighbor level separation s, SYK, t=0.1, 2, 10 for K=0.0001 and K=10, with N=12, 14, 16, 18, 20, 22 and 24. The larger N/2 exponents are used.

this method was applied to the energy spectrum of the SYK model [36], the statistical properties were improved substantially. In this paper, we have used only the fixed-i unfolding for both the SYK model and the XXZ model. The sample-by-sample rescaling slightly changes the results, often bringing the results closer to random matrix or Poisson values, however we did not observe a qualitative change.

# Dependence on N for the SYK model

In Fig. 7, the nearest neighbor level separation s for the SYK model is plotted, for various values of N. When K is close to zero, GUE and GOE can be seen at sufficiently late time, for  $N \equiv 2, 4, 6$  and  $N \equiv 0 \mod 8$ , respectively. Early-time behaviors are rather different: for  $N \equiv 2, 4, 6$ , GUE can be

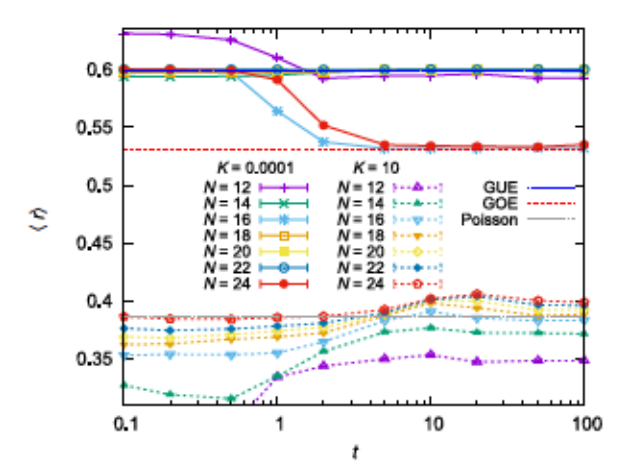


FIG. 8. SYK model, energy eigenstates, the averaged gap ratio as a function of the time t for  $N=12,14,\ldots,24$  for K=0.0001 and  $N=12,14,\ldots,22$  for K=10.

seen from t=0, while for  $N\equiv 0$  substantial deviation from GOE can be seen. Presumably this deviation is related to the exact degeneracy of the exponents at t=0. When K is large, we do not see RMT at all. The nearest gap ratio  $\langle r \rangle$  plotted in Fig. 8 shows the same pattern.

# Dependence on $N_{\text{site}}$ for the XXZ model

In Fig. 9, we have plotted the distribution of the nearest neighbor level separation for  $N_{\rm site}=8,10,12$  and 14. We can see the GOE distribution in the chaotic phase at late time (t=100 in the plots), while the distribution is close to Poisson in the MBL phase. Note that the chaotic phase is not described by RMT at early time. Indeed, at t=0.1, we can see small but non-negligible deviation from RMT. Interestingly, the deviation from RMT becomes large at  $1 \lesssim t \lesssim 10$ , but it eventually vanishes. This deviation at intermediate time becomes larger at larger  $N_{\rm site}$ .

The nearest gap ratio  $\langle r \rangle$  for the central 10% of eigenstates is plotted in Fig. 4 in the main text. In Fig. 10 we also plot the value of  $\langle r \rangle$  averaged over the entire energy spectrum for comparison. The better agreement to the value for GOE at  $1 \lesssim t \lesssim$  20 for W=0.5 should be a coincidence, because as in Fig. 9, the distribution of nearest-neighbor level separations significantly deviates from that for GOE at these times.

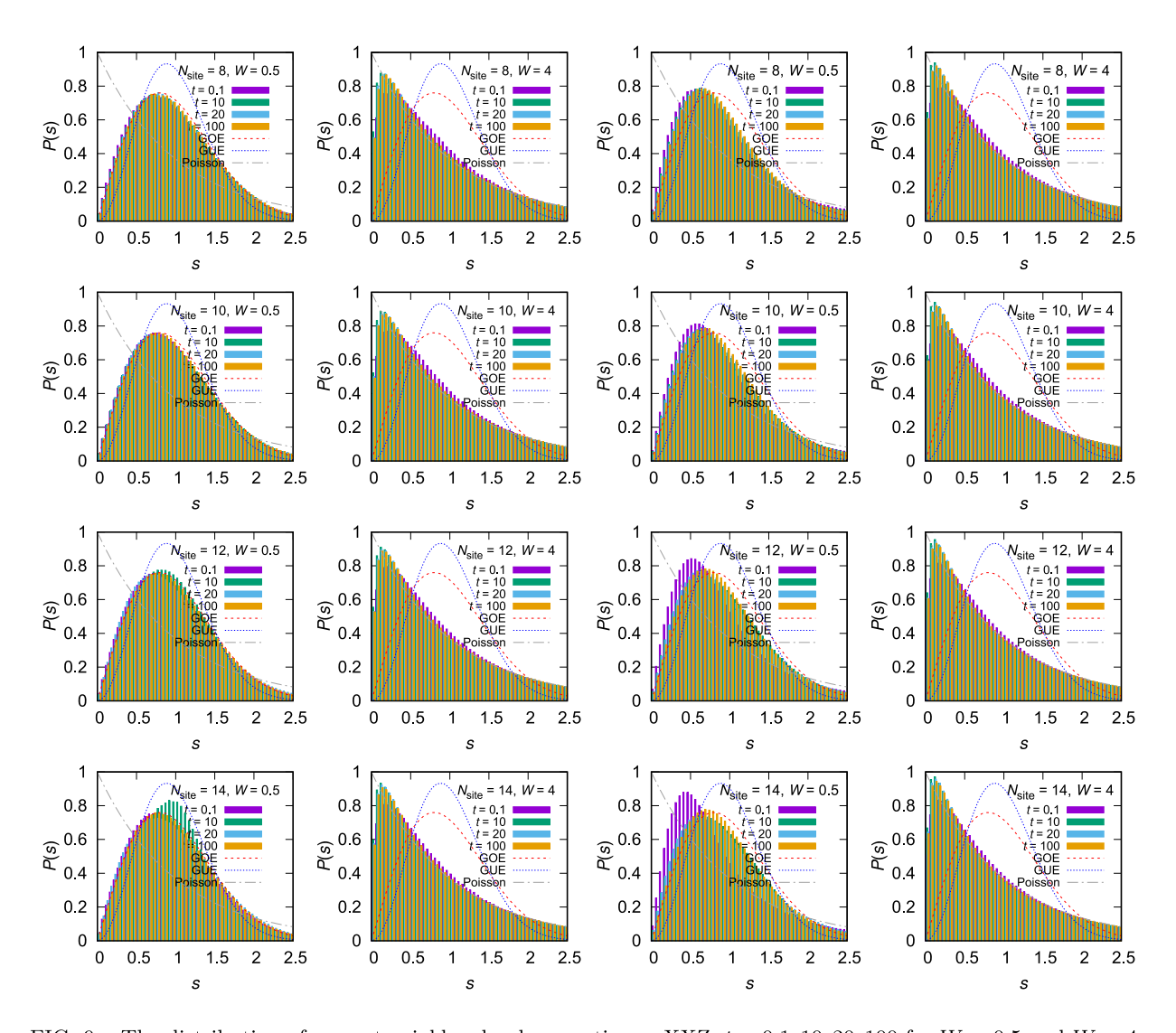


FIG. 9. The distribution of nearest-neighbor level separation s, XXZ, t=0.1, 10, 20, 100 for W=0.5 and W=4, with  $N_{\rm site}=8, 10, 12$  and 14. The larger  $N_{\rm site}/2$  exponents are used. Left two columns: 45% - 55%, right two columns: 0% - 100%. Rescale and shift method is not used, only the fixed-i unfolding has been used.

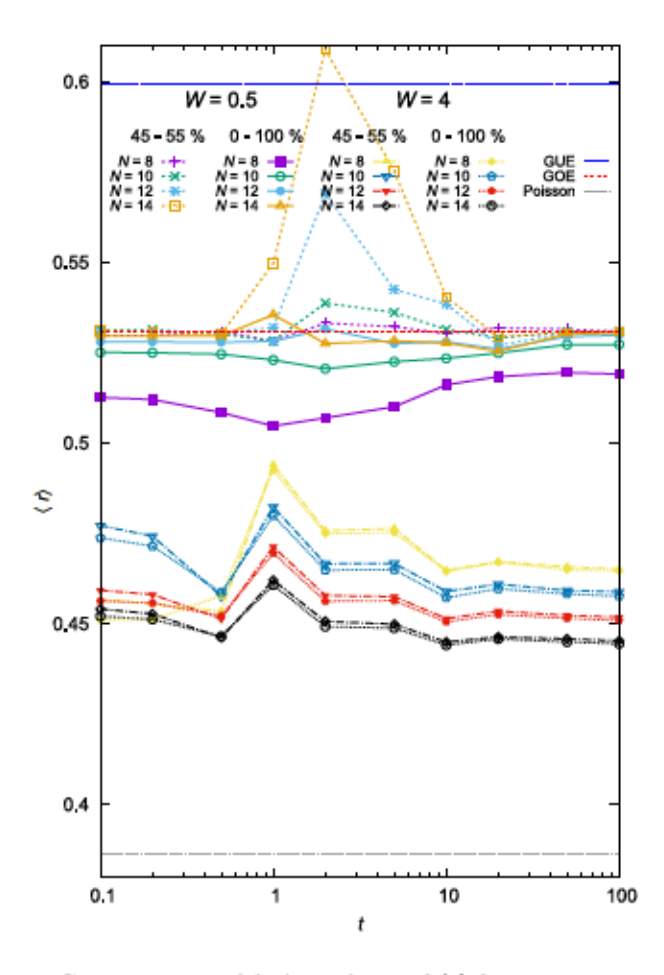


FIG. 10. XXZ model, dependence of  $\langle r \rangle$  for  $N_{\rm site} = 14$  and W = 0.5, 4, using different numbers of eigenstates (central 10% of the eigenstates or all eigenstates for each sample). The larger  $N_{\rm site}/2$  exponents are used. In the figure,  $N_{\rm site}$  is shown as N for brevity.